Flyback Converter with Hybrid Clamp

Laszlo Huber and Milan M. Jovanović
Delta Power Electronics Laboratory
Delta Products Corporation
Research Triangle Park, NC, USA

Haibin Song, Daofei Xu, and Alpha Zhang
Shanghai Design Center
Delta Electronics Shanghai
Shanghai, China

Chien-Chung Chang
Mobile Power Business Group
Delta Electronics, Inc.
Chungli, Taiwan

***Abstract*— This paper presents a flyback converter with a hybrid clamp, i.e., a combined passive RCD and active clamp, and a corresponding power management circuit that substantially optimizes the performance of the flyback converter in the entire line and load ranges. By sensing the operating conditions, the power management circuit configures the clamp circuit either as a passive clamp or as an active clamp. In the passive-clamp configuration, the clamp switch is kept turned off and the main switch turns on with valley switching, whereas, in the active-clamp configuration, the clamp switch operates with pulse-width modulation (PWM) which enables zero-voltage-switching (ZVS) turn-on of the main switch. Performance of the flyback converter with the hybrid clamp is evaluated on a laboratory prototype of a 65-W (19.5-V, 3.33-A) universal-line-voltage-range (90-264 Vrms) adapter.**

Keywords—RCD clamp, active clamp, hybrid clamp, flyback converter, power management

I. INTRODUCTION

The increasing demand for size reduction of today's external power supplies such as adapters/chargers for laptops, tablets, mobile devices, game consoles, printers, etc., has stimulated substantial development and research efforts in high-efficiency and high-power-density power conversion. As the silicon-based devices approach their theoretical performance limit, their ability to improve the performance of the next generation of power supplies is diminished. The emerging wide-band-gap devices, such as GaN-based devices, will inevitably bring about future significant incremental efficiency improvements. Generally, GaN MOSFETs have considerably lower gate charge and lower output capacitance than Si MOSFETs and, therefore, they have a good potential for operation at higher switching frequencies and, consequently, for size reduction of the power supplies. [1]-[4].

In low-power offline applications, the flyback topology is the mostly used topology due to its simplicity and low cost. An integral part of the flyback converter is the clamp circuit that processes the energy stored in the leakage inductance of the flyback transformer after the main switch is turned off. Generally, the flyback topology can be implemented with different clamp structures. The two most employed clamp structures are the RCD clamp [5]-[9] and the active clamp [11]-[16], shown in Figs. 1 and 2, respectively.

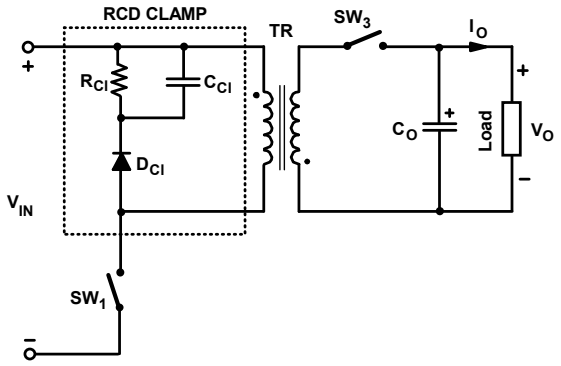

Fig. 1 Flyback converter with RCD clamp.

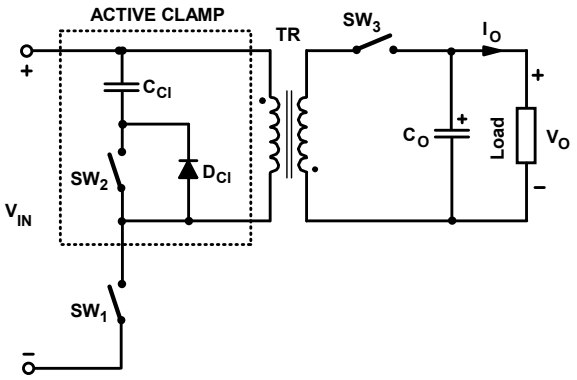

Fig. 2 Flyback converter with active clamp.

In the RCD clamp, the energy stored in the leakage inductance of the flyback transformer is dissipated in the clamp resistor, whereas in the active clamp this energy is recycled and used to achieve zero-voltage-switching (ZVS) turn-on of the main switch. If the flyback converter with active clamp operates with non-complimentary control [13], [15], i.e., when the clamp switch is turned on only for a short time before the main switch is turned on, ZVS can also be achieved at lighter loads when the flyback converter operates in discontinuous-conduction mode (DCM). It should be noted that with the RCD clamp, ZVS turn-on of the main switch can be achieved only at input voltages V_{IN} which are lower than the primary-side reflected output voltage NV_O, where N is the ratio of the number of primary-winding turns and the number of secondary-winding turns, and V_O is the output voltage. Therefore, due to ZVS and the leakage energy recycling, the active clamp generally exhibits better performance than the RCD clamp at heavier loads and higher input voltages ($V_{IN} > NV_O$). However, at very light loads, where the flyback converter operates in deep DCM and the active-clamp switch turns on when the resonance between the magnetizing inductance of the flyback transformer and the circuit parasitic capacitances is almost completely damped out, the turn-on loss of the active-clamp switch at low input voltages is greater than the loss saved by ZVS turn-on of the main switch, i.e.,

$$\frac{1}{2}C_{eq}(NV_O)^2 f_{SW} + V_{GG} Q_{Gate} f_{SW} > \frac{1}{2}C_{eq}(V_{IN})^2 f_{SW} \quad , \quad (1)$$

where, C_{eq} is the equivalent parasitic capacitance of switches SW_1 and SW_2, the primary-side reflected parasitic capacitance of switch SW_3 , and the parasitic winding capacitance of the flyback transformer; f_{SW} is the switching frequency; V_{GG} is the gate drive voltage of switch SW_2, and Q_{Gate} is the total gate charge of switch SW_2. Since at very light loads the energy stored in the leakage inductance of the flyback transformer is practically negligible, the performance of the flyback converter with RCD clamp at very light loads and low input voltages $V_{IN} < NV_O$ may be better than that with the active clamp.

Therefore, the performance of the flyback converter in the entire line and load ranges can be optimized by combining the RCD clamp and the active clamp into a hybrid clamp.

II. Hybrid-Clamp Topology and Control

The circuit diagram of the flyback converter with a hybrid clamp is presented in Fig. 3. As shown in Fig. 3, the clamp circuit, which is connected in parallel to the primary winding of the flyback transformer *TR*, comprises a parallel combination of clamp capacitor C_{Cl} and clamp resistor R_{Cl} that is connected in series with a parallel combination of switch SW_2 and clamp diode D_{Cl}. Fig. 3 also shows a control block, which includes a controller and a power management unit. The controller provides the control signals for main switch SW_1, clamp switch SW_2, and synchronous rectifier switch SW_3, if any, to regulate the output voltage. The power-management unit generates the enable/disable signal for clamp switch SW_2 based on the converter's operating conditions. When signal EN is LOW, the clamp circuit is configured as a passive clamp (PCL), i.e., clamp switch SW_2 is kept turned off. However, when signal EN is HIGH, the clamp circuit is configured as an active clamp (ACL)

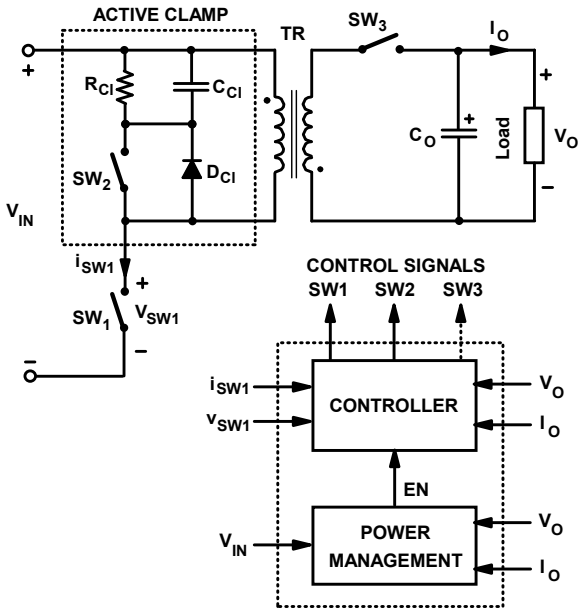

Fig. 3 Flyback converter with hybrid clamp.

and clamp switch SW_2 is switched at the same frequency as main switch SW_1 so that switch SW_1 turns on at ZVS. During this mode of operation, switches SW_1 and SW_2 never conduct at the same time, i.e., switch SW_2 is turned on during the off-time of switch SW_1 and vice versa.

It should be noted that the controller and the power management unit can be implemented by hardware, software, or any combination of hardware and software. Generally, a hardware implementation includes analog and digital circuits, while a software implementation includes one or more microcontrollers, digital-signal processors, or both, that execute the algorithms that constitute the controller and the power management unit.

Switches SW_1, SW_2, and SW_3 in Fig. 3 can be implemented with Si MOSFET switches and/or GaN and SiC switches. Clamp diode D_{Cl} in Fig. 3 can be implemented by using the body diode of MOSFET clamp-switch SW_2 or by an external diode. It should be noted that the hybrid-clamp circuit can also be implemented by connecting it in parallel to the primary switch SW_1.

Principle of operation of the hybrid-clamp circuit is illustrated in Figs. 4 and 5. Figure 4 shows, as an example, desired regions of operation for the passive-clamp and active-clamp circuits in the I_O-V_{IN} plane. The boundary between the two regions, shown with the dashed line, is determined by preferred optimization criteria such as, for example, maximum efficiency. If, for example, the input voltage V_{IN} and the output current I_O of the flyback converter correspond to operating point "A" in Fig. 4, i.e., the operating point is in the region where the passive-clamp (PCL) operation is optimal, the power management block in Fig. 3 will generate EN = LOW signal and the flyback converter will operate with the clamp circuit configured as the passive clamp where only main primary switch

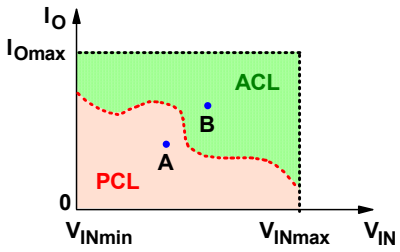

Fig. 4 Regions of operation for passive-clamp and active-clamp circuits in I_O-V_{IN} plane.

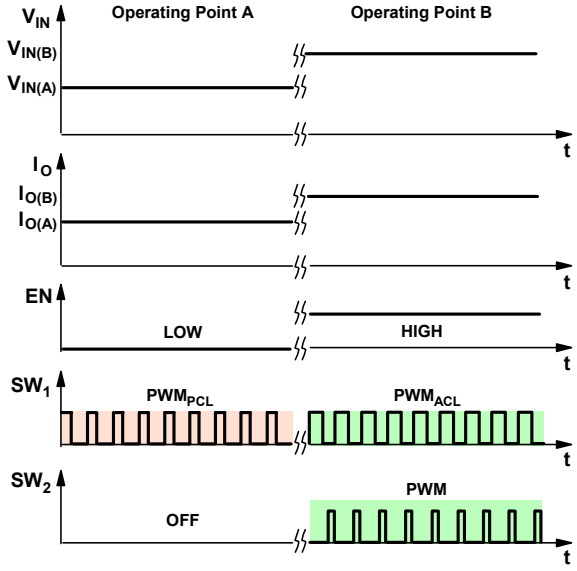

Fig. 5 Principle of operation of flyback converter with hybrid clamp.

SW_1 is modulated, as shown in Fig. 5. However, if the input voltage V_{IN} and the output current I_O of the flyback converter correspond to operating point "B" in Fig. 4, i.e., the operating point is in the region where the active-clamp (ACL) operation is optimal, the power management block in Fig. 3 will generate EN = HIGH signal and, consequently, the flyback converter will operate with the clamp circuit configured as the active-clamp where both primary switch SW_1 and SW_2 are modulated, as also illustrated in Fig. 5.

Generally, the desired regions of operations for the passive-clamp and active-clamp operation can be determined based on any arbitrary design optimization criteria. For example, besides efficiency, these regions can also be determined based on electromagnetic interference (EMI), component-stress, and/or transformer performance optimization considerations. The desired regions of operation can be determined analytically, i.e., by calculations and/or simulations, and/or by measurements on a prototype circuit. In both approaches, the desired optimization quantity is evaluated for a set of operating points for both the passive- and active-clamp operations to determine which operation exhibits better performance. Based on this evaluation, the boundary between passive- and active-clamp regions of operation can be defined and employed in the power-management algorithm. For example, in a digital implementation, the boundary operating points may be stored in a look-up table so that the power-management algorithm tests the actual operating point of the converter with respect to the boundary operating points to determine the region of operation, i.e., to determine which clamp method is optimal.

III. Performance Evaluation

Performance of the flyback converter with the hybrid clamp is evaluated on a 65-W (19.5-V, 3.33-A) adapter prototype for the universal line-voltage range (90-264 Vrms). The circuit diagram of the experimental circuit along with component information is presented in Fig. 6. The minimum input voltage after the line-voltage rectifier is $V_{IN,min} = 88$ V, which is obtained at 90-Vrms line voltage with a 120-µF bulk capacitor at full load. The maximum input voltage after the line-voltage rectifier is $V_{IN,max} \approx 375$ V, which is obtained at the peak value of 264-Vrms line voltage. All experimental results, presented in Figs. 7-15, are obtained at dc input voltages $V_{IN} = 88$-375 V.

It should be noted that in the active-clamp mode, the circuit operates with non-complimentary control [13], [15].

Key measured waveforms obtained with hybrid clamp in PCL mode at minimum input voltage $V_{IN,min} = 88$ V, at 100%, 10%, and 5% load are shown in Figs. 7, 8, and 9, respectively. The corresponding waveforms obtained with hybrid clamp in ACL mode are shown in Figs. 10, 11, and 12, respectively. The waveforms obtained with hybrid clamp in PCL mode in Fig. 7 and Figs. 8 and 9, illustrate the ZVS switching at full load and valley switching at 10% and 5% loads, respectively. The corresponding waveforms obtained with hybrid clamp in ACL mode in Figs. 10, 11, and 12, show that ZVS switching is achieved in the entire load range. The drain-source voltage waveform of the main switch in Figs. 11 and 12 illustrate that in active clamp mode the circuit operates with non-complimentary control.

DC-DC efficiency $\eta_{DC\text{-}DC} = P_O/P_{IN}$ measurements at 100%, 10%, and 5% load are presented in Figs. 13, 14, and 15, respectively. As shown in Figs. 13-15, by combining the RCD clamp and the active clamp into a hybrid clamp, the efficiency

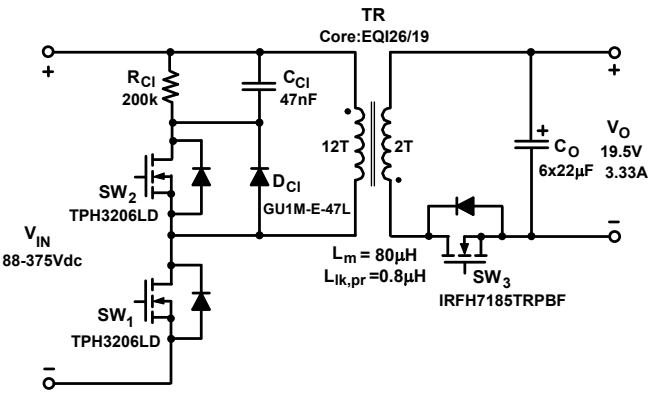

Fig. 6 Experimental circuit.

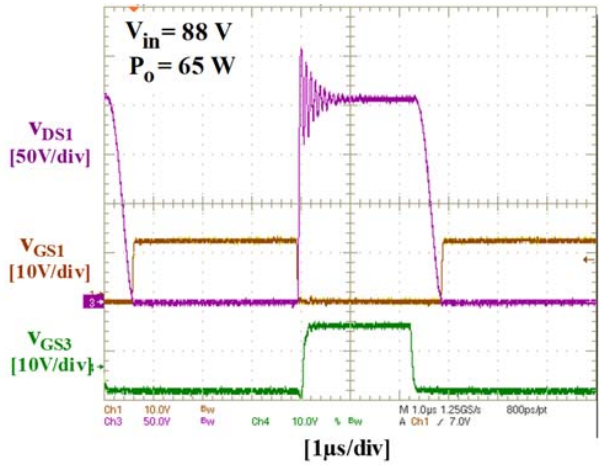

Fig. 7 Measured waveforms obtained with hybrid clamp in PCL mode at 88-V input voltage and 100% load.

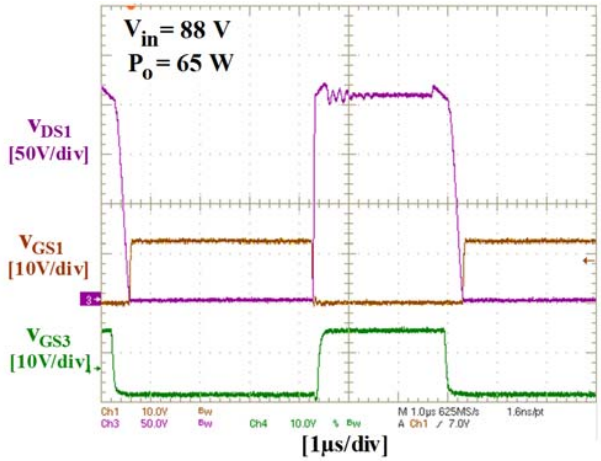

Fig. 10 Measured waveforms obtained with hybrid clamp in ACL mode at 88-V input voltage and 100% load.

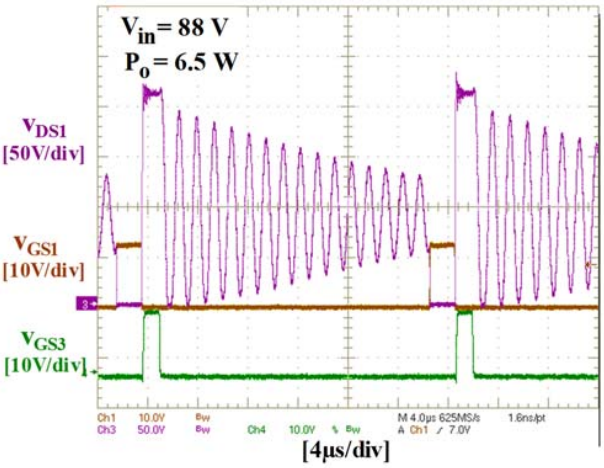

Fig. 8 Measured waveforms obtained with hybrid clamp in PCL mode at 88-V input voltage and 10% load.

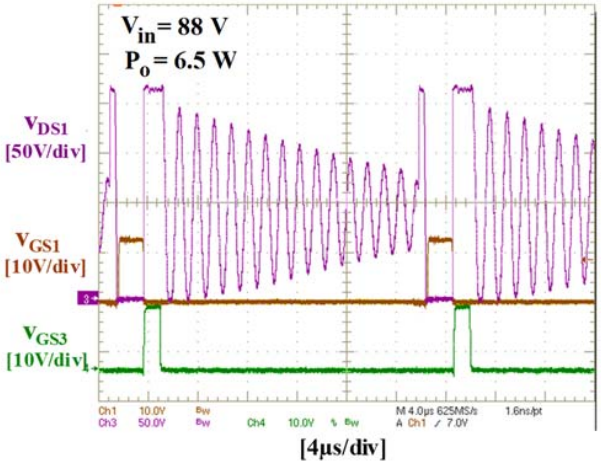

Fig. 11 Measured waveforms obtained with hybrid clamp in ACL mode at 88-V input voltage and 10% load.

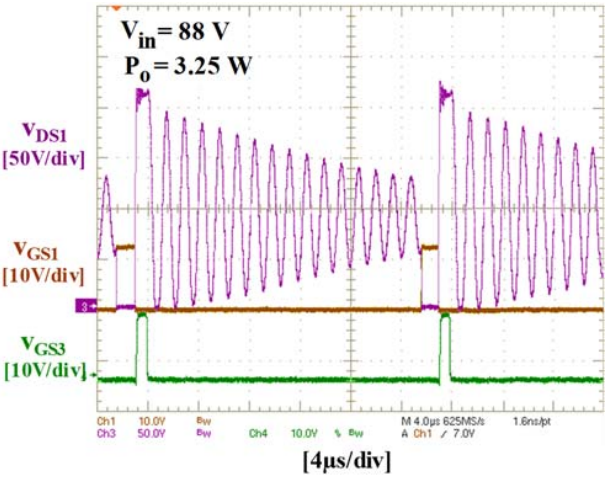

Fig. 9 Measured waveforms obtained with hybrid clamp in PCL mode at 88-V input voltage and 5% load.

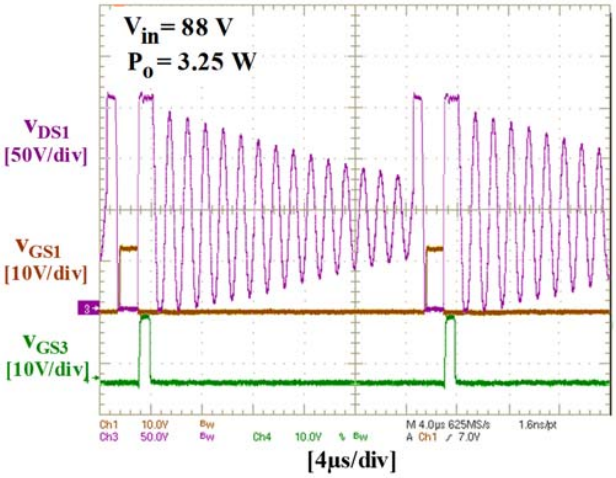

Fig. 12 Measured waveforms obtained with hybrid clamp in ACL mode at 88-V input voltage and 5% load.

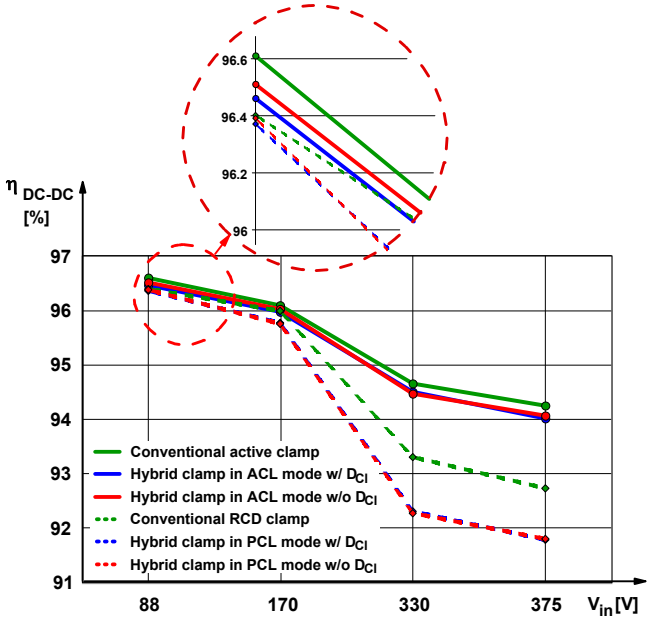

Fig. 13 Efficiency measurements at 100% load.

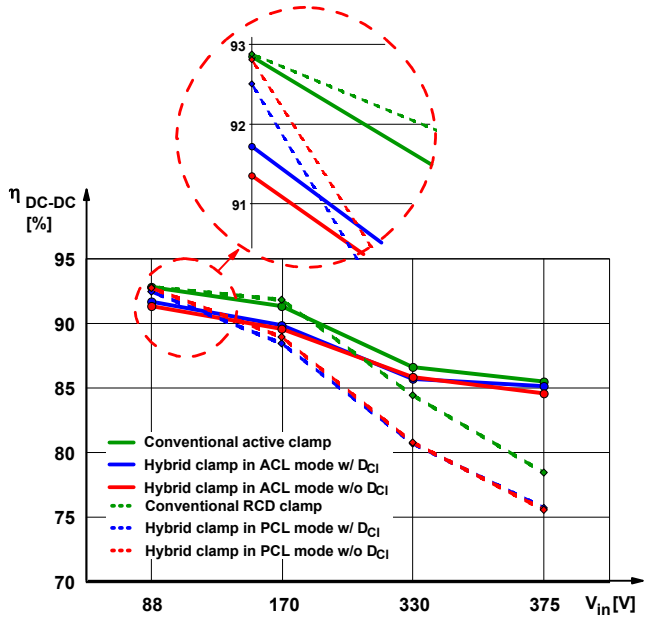

Fig. 14 Efficiency measurements at 10% load.

of the flyback converter is slightly compromised, i.e., the flyback converter with the hybrid clamp in ACL mode has slightly lower efficiency than the flyback converter with the conventional active clamp, which is the result of the additional loss in the clamp resistor added in parallel to the conventional clamp capacitor. For example, at 100% load, the maximum

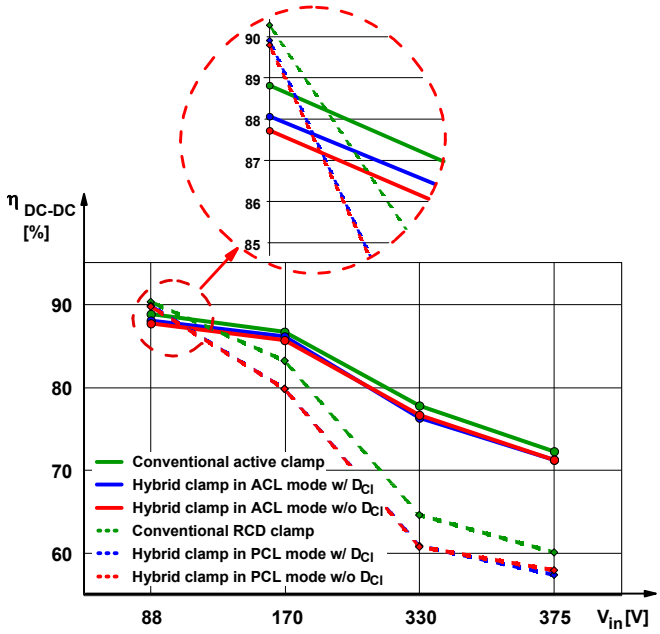

Fig. 15 Efficiency measurements at 5% load.

efficiency reduction is around 0.2% at maximum input voltage $V_{IN,max}$ = 375 V (solid lines in Fig. 13). Similarly, the flyback converter with the hybrid clamp in PCL mode has slightly lower efficiency than the flyback converter with the conventional RCD clamp, which is the result of the additional turn-on loss due to the capacitance of the clamp switch connected in parallel to the conventional clamp diode. This effect is more pronounced at higher input voltages. For example, at 100% load, the maximum efficiency reduction is around 0.9% at maximum input voltage $V_{IN,max}$=375 V (dashed lines in Fig. 13). At 100% load, as shown in Fig. 13, the flyback converter with the hybrid clamp in ACL mode is more efficient than its PCL mode counterpart in the whole input voltage range. At 10% load, as shown in Fig. 14, the flyback converter with the hybrid clamp in PCL mode becomes more efficient than its ACL mode counterpart in a narrow input voltage range at the minimum input voltage. Specifically, at minimum input voltage $V_{IN,min}$=88 V, the efficiency in PCL mode without clamp diode D_{Cl} is 92.81% versus 91.35% in corresponding ACL mode. However, this efficiency is still lower than the efficiency of the flyback converter with the conventional active clamp (92.85%). Finally, at 5% load, as shown in Fig. 15, the flyback converter with the hybrid clamp in PCL mode in a very narrow input voltage range at the minimum input voltage becomes more efficient even than the flyback converter with the conventional active clamp. Specifically, at minimum input voltage $V_{IN,min}$=88 V, the efficiency in PCL mode with clamp diode D_{Cl} is 89.91% versus 88.81% of the conventional active clamp and 88.07% in corresponding ACL mode.

IV. Conclusion

The hybrid clamp helps to optimize the performance of the flyback converter in the entire line and load ranges. The hybrid clamp in the ACL mode exhibits better performance than in the PCL mode in most parts of the I_O-V_{IN} plane. However, at light loads approximately below 10% of full load and at low input voltages in a narrow range at the minimum input voltage (approximately between 88 V and 120 V), the performance of the flyback converter with the hybrid clamp in the PCL mode is better than that of its ACL mode counterpart.

References

[1] M.A. Khan, G. Simin, S.G. Pytel, A. Monti, E. Santi, and J.L. Hudgins, "New development in Gallium Nitride and the impact on power electronics," *Proc. Power Electronics Specialists Conf. (PESC)*, Jun. 2005, pp. 15-16.

[2] N. Ikeda, Y. Niiyama, H. Kambayashi, Y. Sato, T. Nomura, S. Kato, and S Yoshida, "GaN power transistors on Si substrates for switching applications," *Proc. IEEE*, vol. 98, no. 7, pp. 1151-1161, Jul. 2010.

[3] X. Huang, Z. Liu, Q. Li, and F.C. Lee, "Evaluation and application of 600 V GaN HEMT in cascode structure," *IEEE Trans. Power Electronics*, vol. 29, no 5, pp. 2453-2461, May 2014.

[4] X. Huang, Z. Liu, F.C. Lee, and Q. Li, "Characterization and enhancement of high-voltage cascode GaN devices," *IEEE Trans. Electron Devices*, vol. 62, no 2, pp. 270-277, Feb. 2015.

[5] L. Huber and M.M. Jovanović, "Evaluation of flyback topologies for notebook AC/DC adapter/charger applications," *Proc. High Frequency Power Conversion Conf. (HFPC)*, pp. 284-294, May 1995.

[6] G. Koo, "Design guidelines for RCD snubber of flyback converters," *Application Note* AN-4147, Fairchild Semiconductor, 2006.

[7] P. Meng, X. Wu, J. Yang, H. Chen, and Z. Qian, "Analysis and design considerations for EMI and losses of RCD snubber in flyback converter, *Proc. Applied Power Electronics Conf. (APEC)*, pp. 642-647, Feb. 2010.

[8] C. Wang, S. Xu, S. Lu, and W. Sun, "An accurate design method of RCD circuit for flyback converter considering diode reverse recovery," *Proc. Int'l Conf. on Industrial Technology (ICIT)*, pp. 268-274, Mar. 2016.

[9] S. Liu, F. Zhang, and Q. Zhang, "Optimal design of RCD parameters in flyback converter," *Proc. Int'l Symp. on Computer, Consumer and Control*, pp. 583-586, Jul. 2016.

[10] K. Yoshida, T. Ishii, and N. Nagagata, "Zero voltage switching approach for flyback converter," *Proc. Int. Telecomm. Energy Conf. (INTELEC)*, pp. 324-329, Oct. 1992.

[11] R. Watson, F.C. Lee, and G. Hua, "Utilization of an active-clamp circuit to achieve soft switching in flyback converters," *IEEE Trans. Power Electronics*, vol. 11, no 1, pp. 162-169, Jan. 1996.

[12] P. Alou, O. Garcia, J.A. Cobos, J. Uceda, and M. Rascon, "Flyback with active clamp: a suitable topology for low power and very wide input voltage range applications," *Proc. Applied Power Electronics Conf. (APEC)*, pp. 242-248, Mar. 2002.

[13] J. Zhang, X. Huang, X. Wu, and Z. Qian, "A high efficiency flyback converter with new active clamp technique," *IEEE Trans. Power Electronics*, vol. 25, no 7, pp. 1775-1785, Jul. 2010.

[14] X. Huang, J. Feng, W. Du, F.C. Lee, and Q. Li, "Design considerations of MHz active clamp flyback converter with GaN devices for low power adapter applications," *Proc. Applied Power Electronics Conf. (APEC)*, pp. 2334-2341, Mar. 2016.

[15] J.M. Zhang and X.C. Huang, ZVS flyback DC-DC switch-mode power supply, CN Patent 101572490A, Nov. 4, 2009.

[16] J.J. Zhang and D.M. Kinzer, Zero voltage soft switching scheme for power converters, US Patent 9621044 B2, Apr. 11, 2017.